Magnetic Resonance Imaging of the Peripheral Nerve

5

Roberto Gasparotti and Massimiliano Filosto

5.1 Introduction

The diagnostic workup of peripheral neuropathies has traditionally relied on the patient's clinical history, physical examination, and electrophysiological studies [1].

Clinical and instrumental data usually provide enough information about the location, severity, as well as the etiology of the underlying nerve injury in the majority of patients. However, electrodiagnostic studies do not display the anatomic detail needed for precise localization and treatment planning, therefore imaging techniques, especially Magnetic Resonance Imaging (MRI) and nerve ultrasound (US), are gaining an increasing role in the evaluation of peripheral neuropathies [2, 3].

In conventional MRI studies, peripheral nerves are poorly visualized due to low contrast resolution between nerves, muscles and vessels, signal intensity variability, pulsatility artifacts, and small size. These disadvantages have been overcome with the development of Magnetic Resonance Neurography (MRN) in the 1990s [4, 5].

DTI is a functional MRI technique that represents a new source of information about the microstructural integrity of peripheral nerves, allowing quantitative measurements which have been proved useful for further characterization of neuropathies with different etiologies [6].

Ultrasound (US) is very suitable for dynamic assessment of the abnormalities of superficial peripheral nerves, such as changes in nerve caliber, continuity, and echogenicity and represents a useful complement of clinical and

R. Gasparotti (✉)
Section of Neuroradiology, Department of Medical and Surgical Specialties, Radiological Sciences and Public Health, University of Brescia, Brescia, Italy
e-mail: roberto.gasparotti@unibs.it

M. Filosto
Department of Clinical and Experimental Sciences, NeMO-Brescia Clinical Center for Neuromuscular Diseases, University of Brescia, Brescia, Italy
e-mail: massimiliano.filosto@unibs.it

C. Angelini (ed.), *Acquired Neuromuscular Disorders*,
https://doi.org/10.1007/978-3-031-06731-0_5

electrophysiological evaluation [7], although it is more operator-dependent than MRI, and less effective in cases of deeply situated nerves, especially of the pelvis and lumbosacral plexus.

5.2 Magnetic Resonance Neurography

MRN is a tissue-selective imaging technique, based on T2-weighted sequences with fat suppression, acquired with dedicated surface coils and small field of view, which is directed at identifying and evaluating specific characteristics of nerve morphology, such as internal fascicular pattern, longitudinal variations in signal intensity and caliber, and connections and relations to other nerves or plexuses [8].

The most efficient method of fat suppression is with T2-weighted Short Time Inversion Recovery (STIR) sequences, which provide a selective suppression of the fat signal using an inversion recovery pulse of 150 ms. These sequences, however, have some disadvantages, mainly represented by poor signal-to-noise ratio and pulsatility artifacts caused by vessels. Alternative methods for fat suppression are represented by T2 spectral adiabatic inversion recovery imaging (SPAIR) or DIXON-type fat suppression, which are both characterized by a better signal-to-noise ratio, although the contrast resolution is lower [9].

In order to obtain the best compromise between spatial resolution, field of view (FOV) and acquisition time, MRN sequences should be adapted to the anatomical region and the best echo time should be carefully selected in order to obtain a satisfactory differentiation between nerves and muscles, as the signal intensity of the nerve is very sensitive to small changes (Fig. 5.1).

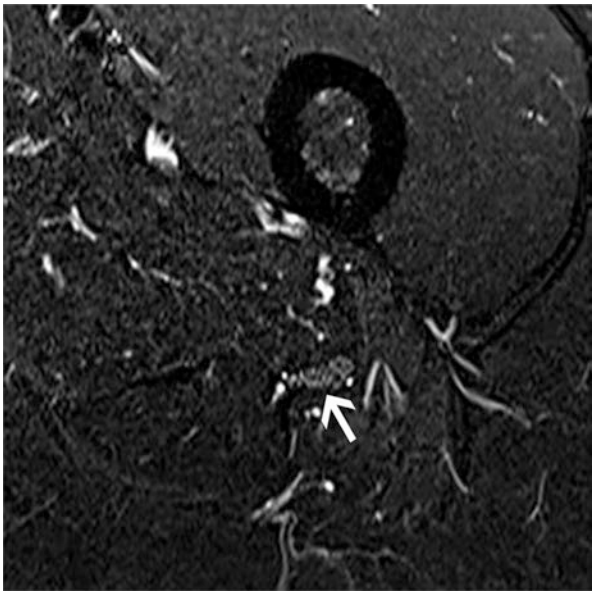

Fig. 5.1 MRN (1.5T), axial T2-STIR section at mid-thigh. Normal subject. The right sciatic nerve (arrow) is moderately hyperintense compared to the adjacent muscles and its transverse fascicular pattern is clearly identifiable

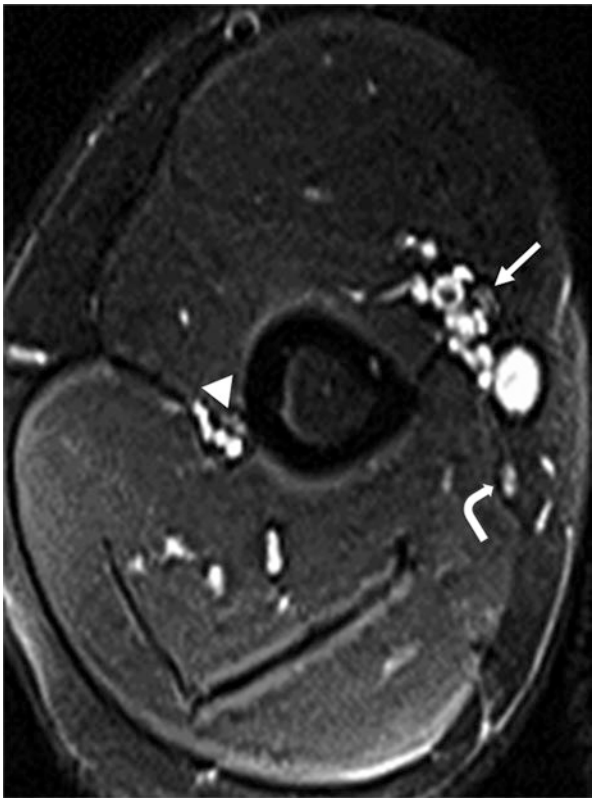

Fig. 5.2 MRN (3T), axial T2-STIR section at mid-humerus. Normal subject. The median (arrow), ulnar (curved arrow) and radial (short arrow) nerves, which are moderately hyperintense, can be differentiated from adjacent muscles and vessels

Recent technological advances, such as parallel imaging, new coil design and new sequences, together with an increasing use of 3T MR scanners, have led to the development of high-resolution MR peripheral nerve imaging, which provides significantly better depiction of peripheral nerve structures [10] (Fig. 5.2).

Three-dimensional (3D) MRN represents a further refinement of conventional MRN. 3D sequences provide enhanced contrast between nerves and muscles and are typically acquired with isotropic voxels, therefore conferring the advantage of generating oblique and curved-planar reformations of nerve roots, peripheral nerves, and plexuses [11]. Excellent contrast of the nerves can be obtained by suppressing muscle, blood and fat signal with fat-suppressed diffusion-prepared 3D MR Neurography sequences [12]. These features are particularly useful for imaging the anatomical complexity of brachial and lumbosacral plexuses which cannot be fully displayed by 2D imaging [13] (Fig. 5.3).

In MRN studies, normal nerves are identifiable as rounded or ovoid structures on axial images, are typically isointense to slightly hyperintense on T2-weighted images, depending on the size of the nerve, on the amount of endoneurial fluid and degree of fat suppression, whereas they are isointense to the adjacent muscles on conventional T1-weighted images [14].

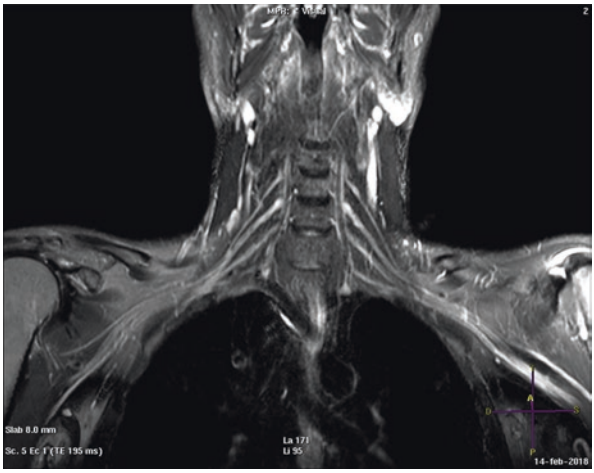

Fig. 5.3 3D MRN (3T) of the brachial plexus. Oblique coronal reformat. The supra and infraclavicular brachial plexus is simultaneously displayed in a single image

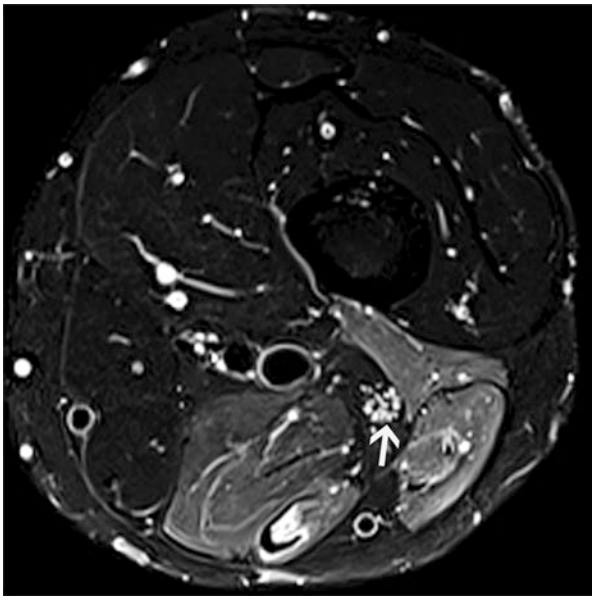

Fig. 5.4 MRN (1.5T), axial T2-STIR section of the left thigh. A 38-year-old male with left sciatic nerve injury. Enlargement and hyperintensity of the left sciatic nerve, which is characterized by fascicular hypertrophy (arrow). Increased signal intensity of semimembranosus, semitendinosus, and long head of the biceps femoris, due to acute denervation

The epineurium appears as a thin hypointense rim and the transverse and longitudinal fascicular pattern may be identified in larger nerves such as the sciatic nerve or the median nerve at the carpal tunnel.

The signal intensity of normal nerves is strongly influenced by the amount of collagen fibers contained in the perineurium and endoneurium and their magnetic properties, which depend on the angle with the principal vector of the magnetic field, and this concept should be taken into account in the image interpretation [15].

Diseased nerves become hyperintense to muscle on MRN images and are focally or globally enlarged [16] (Fig. 5.4).

The signal intensity change is due to increased water content in the epineurial space caused by blood–nerve barrier damage, blockade of axoplasmic flow, inflammation, distal Wallerian degeneration and is relatively independent from the etiology of the neuropathy [17].

Neuropathies with different etiologies cannot be distinguished only on the basis of signal intensity changes, as no reliable quantitative methods for evaluating the signal intensity of normal versus abnormal nerves have been developed up to now.

A common method to recognize variations of the size of the nerves is the measurement of the cross- sectional area (CSA) with manually drawn ROIs in the axial sections perpendicular to the course of the nerves. From the same ROI, a relative quantitative assessment of the signal intensity of the nerve can be obtained normalizing its value with the signal intensity of a reference adjacent muscle or with the calculation of nerve-to-muscle contrast-to-noise ratio (CNR) [18].

MRN has the advantage of a simultaneous exploration of nerves and muscles, therefore muscle denervation represents a useful MR sign of peripheral nerve disease (Fig. 5.4).

In the acute phase of muscle denervation increased signal intensity can be observed in T2-weighted sequences as early as 24 h after nerve injury and lasting for more than 2 months [19]. These denervation-related signal abnormalities are reversible and represent enlargement of the capillary bed and shift of fluid to the extracellular space. In the subacute phase, a progressive decrease of signal intensity is associated with an initial fat replacement, and in chronic phase muscles show atrophy and sever fat replacement, which is better displayed by T1-weighted images.

The observed MR changes precede the earliest EMG findings of denervation, which are not detectable until the second week, thus MR imaging may be useful in narrowing this diagnostic gap.

Diffusion Tensor Imaging (DTI) is a novel technique which has been recently applied to the investigation of peripheral nerve disorders. Nerves are characterized by greater water diffusion anisotropy compared to the surrounding tissues. These techniques are sensitive to subtle changes in tissue at the microstructural level and allow measurement of nerve microstructural integrity based on quantitative parameters such as Fractional Anisotropy (FA), Mean Diffusivity (MD), Axial Diffusivity (AD), and Radial Diffusivity (RD) [20].

Peripheral nerve tractography is increasingly used for selective visualization of peripheral nerves. With the same approach used in deterministic tractography of the brain white matter, seed points placed on the nerves with the aid of a reference anatomical image, allow successful tracking of major peripheral nerves (Fig. 5.5).

DTI has been extensively applied to the investigation of the median, ulnar and radial nerves at the arm [21–23] and more recently to the brachial and lumbosacral plexus with the aim to obtain quantitative measurements potentially useful for more precise imaging characterization of immune-mediated neuropathies.

A comprehensive MRI protocol for the investigation of peripheral nerves should include MRN, which provide both structural and functional information on the nerves and muscle denervation, T1-weighted sequences which are helpful for a precise anatomical identification of nerves and for the identification of muscular

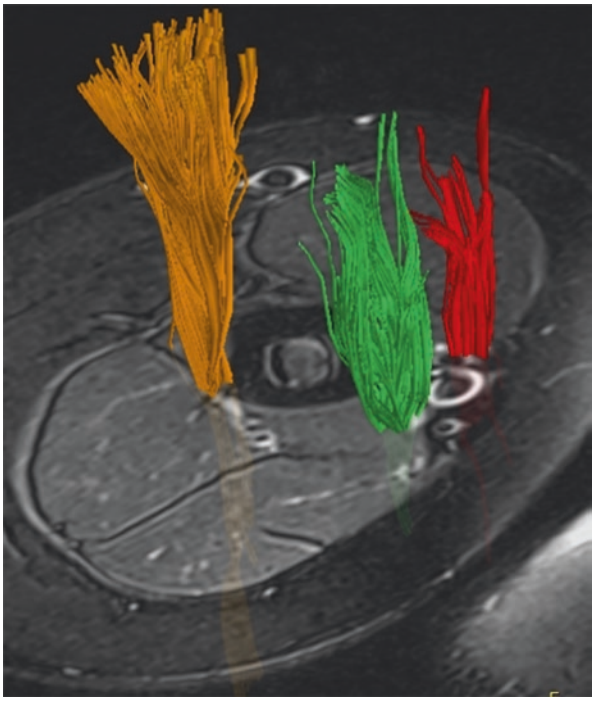

Fig. 5.5 DTI tractography (3T) of median (red), ulnar (green), and radial (orange) nerves at the arm in a normal subject

atrophy and T1-weighted sequences after contrast media administration for the evaluation of the blood–nerve barrier integrity.

MRN has been reported to be effective on the diagnostic workup of traumatic nerve injuries [24], nerve entrapment syndromes [25, 26], and nerve tumors [27]. More recently, MRN has been proposed for the evaluation of hereditary and immune-mediated disorders of peripheral nerves [28], diabetic polyneuropathy [29], and paraproteinemic neuropathies [30].

5.3 Guillain–Barre Syndrome

Guillain–Barre syndrome (GBS) is a well-known inflammatory disease of peripheral nerves, including the spinal and cranial nerves, characterized by albuminocytologic dissociation and demyelinating and/or axonal involvement at electrophysiologic testing.

GBS is divided into different subtypes: acute inflammatory demyelinating polyneuropathy (AIDP), which accounts for 90% of all GBS cases in Western countries and the axonal subtypes, acute motor axonal neuropathy (AMAN), and acute motor and sensory axonal neuropathy (AMSAN), most frequent in Asia and Japan and the Miller-Fisher syndrome (MFS) [31].

MRI studies are usually not necessary for diagnosis although a thorough medical assessment of patients may be needed to exclude "mimic disorders" [32].

Nerve conduction studies (NCS) and CSF analysis are important investigations that help confirming the clinical diagnosis of GBS although NCS may be unrevealing when studying patients within days of symptom onset and CSF may be normal in the first week of the illness [33].

In the initial phase of GBS, breakdown of the blood–nerve barrier is the characteristic pathologic change, which may lead to enhancement of nerve roots in MRI studies.

Although the enhancement of the intrathecal spinal nerve roots is not specific and can be seen in neoplasia and other inflammatory processes, the enhancement of only the anterior spinal nerve roots is strongly suggestive of GBS [34] (Fig. 5.6).

About 5% of patients initially diagnosed with GBS turn out to have chronic inflammatory demyelinating polyradiculoneuropathy (CIDP) with acute onset (A-CIDP) [35].

Differentiating A-CIDP from GBS prior to relapse is challenging at the onset of the disease and has implications for treatment as well as prognosis. Electrodiagnostic

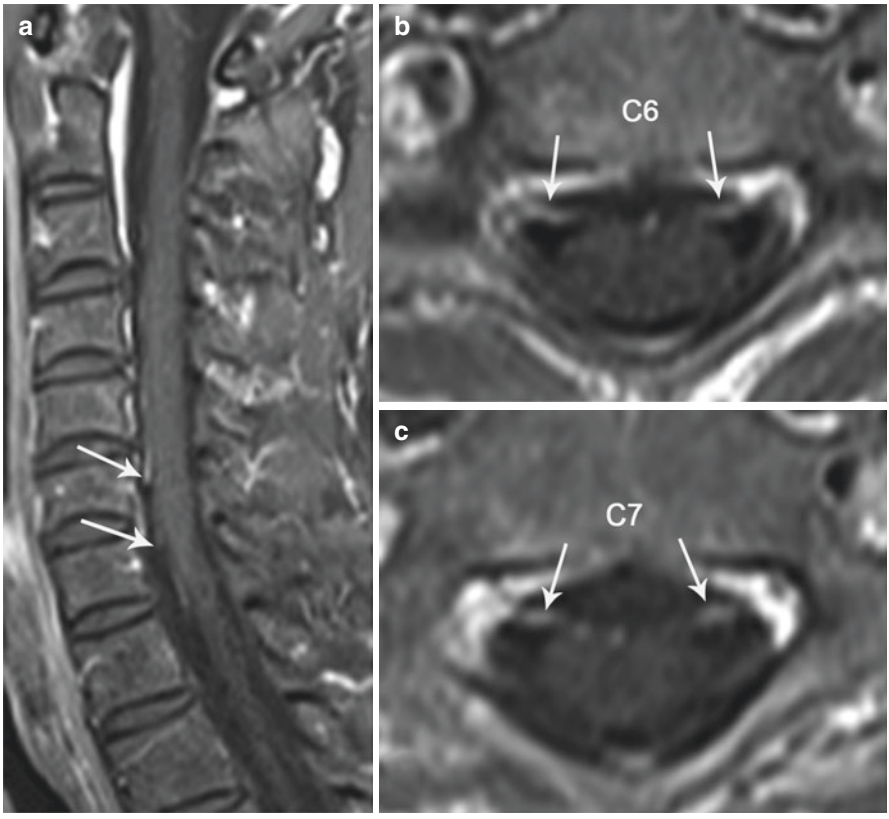

Fig. 5.6 GBS, MR (1.5T), sagittal (**a**), and axial T1-W sections (**b**, **c**) after gadolinium administration. Enhancement of ventral C6 and C7 nerve roots (arrows)

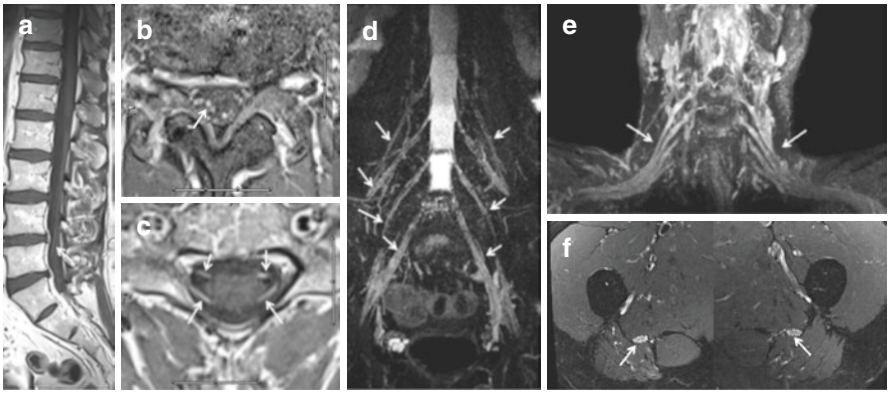

Fig. 5.7 Acute onset CIDP, MR (3T). Sagittal (**a**), axial L3–L4 (**b**), axial C5–C6 (**c**), T1-W sections after gadolinium administration, 3D MRN coronal view, lumbosacral plexus (**d**) and brachial plexus (**e**), axial 2D MRN (**f**), comparative evaluation of sciatic nerves at proximal thigh. Enhancement of cauda equina (arrows in **a** and **b**) and ventral and dorsal C6 nerve roots (arrows in **c**). Symmetric bilateral hypertrophy and increased signal intensity of the lumbosacral and brachial plexus (arrows in **d** and **e**). Increased signal intensity and diffuse fascicular hypertrophy of both sciatic nerves (arrows in **f**)

studies may distinguish patients with A-CIDP from GBS patients; however, the demonstration of brachial and/or lumbosacral plexus hypertrophy at MR imaging may be useful for the differential diagnosis (Fig. 5.7).

5.4 Chronic Immune-Mediated Neuropathies

5.4.1 CIDP

Chronic inflammatory demyelinating polyradiculoneuropathy (CIDP) is an immune-mediated neuropathy characterized by symmetrical proximal and distal weakness, with sensory loss, impaired balance, and areflexia.

CIDP includes a broad spectrum of clinical phenotypes, including atypical forms with pure motor or sensory impairment or distal, multifocal, or focal distributions [36].

The diagnosis of CIDP is based on a combination of clinical, electrodiagnostic, and laboratory features, primarily directed at detecting signs of demyelination; however, in clinical practice CIDP may be difficult to diagnose, especially in atypical cases. Despite the good overall sensitivity and specificity of the current electrophysiological criteria, almost 20% of patients in CIDP cohorts do not match these criteria [37].

MRI showing gadolinium enhancement or hypertrophy of the cauda equina, nerve roots, or plexuses has been recommended as an additional supportive exam in a recent revision of the European Federation of Neurological Societies/Peripheral

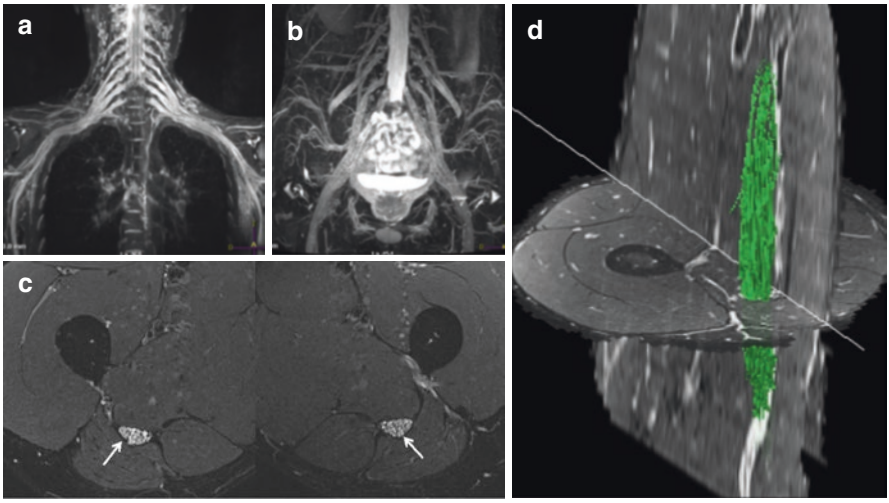

Fig. 5.8 CIDP, 3D MRN (3T), showing diffuse symmetric hyperintensity and enlargement of the brachial (**a**) and lumbosacral plexus (**b**). 2D MRN (**c**) of the proximal thigh, showing symmetric enlargement of sciatic nerves, with diffuse fascicular hypertrophy. DTI tractography of the right sciatic nerve (**d**) with quantitative evaluation of the microstructure of the nerve demonstrated decreased fractional anisotropy (FA, 0.34 vs 0.5) and increased radial diffusivity (RD, 1.5×10^{-3} mm^2/s vs 1.0×10^{-3} mm^2/s) compared to the reference values

Nerve Society guideline on management of CIDP [38] although contrast enhancement is rarely seen in clinical practice.

The most frequent MRI finding in patients affected by CIDP is represented by bilateral and symmetric hypertrophy of both brachial and lumbosacral plexus, which is invariably associated to increased signal intensity, better displayed by MRN (Fig. 5.8).

Hypertrophy and increased signal intensity of the cervical roots and brachial plexus at MRI have been reported in 57% of patients affected by CIDP, 75% of whom also had hypertrophy of the lumbar plexus [39].

Patients with nerve root hypertrophy usually have a relapsing-remitting course and a significantly longer disease duration, which may be related, according to some authors, with the process of demyelination and remyelination [39]. Similar findings of enlargement and increased MR signal intensity have been observed in the median and ulnar nerves of patients with CIDP, correlating with the site of conduction block and contrast-enhancement during relapses or active progression, possibly reflecting increased water content within the nerve fascicles and disruption of the blood–nerve barrier due to the inflammatory process [40].

3D MR Neurography has become a valuable tool for a thorough assessment of the symmetry and longitudinal extent of the disease.

Using 3D MRN techniques Shibuya et al. showed longitudinal morphological changes from the cervical roots to the nerve trunks in the proximal arm in 88% of patients affected by CIDP [41].

Phenotypic features can be noninvasively characterized in patients with atypical variants of CIDP using 3D MRN for a detailed evaluation of brachial and lumbosacral plexus hypertrophy and signal intensity abnormalities, which typically involve long segments with a different distribution, symmetric or asymmetric, diffuse, or multifocal.

Lewis-Sumner syndrome (LSS) or multifocal acquired demyelinating sensory and motor neuropathy (MADSAM) is characterized by asymmetry, presenting as a multifocal multiple mononeuropathy most commonly in the upper limbs, accounting for 6–15% of CIDP patients [37].

The distribution of hypertrophy in typical CIDP is symmetric and predominant in the nerve roots, with gradual normalization toward the proximal arm segments distally, whereas in MADSAM nerve hypertrophy is usually asymmetric and multifocal in the peripheral nerve trunks [42] (Fig. 5.9).

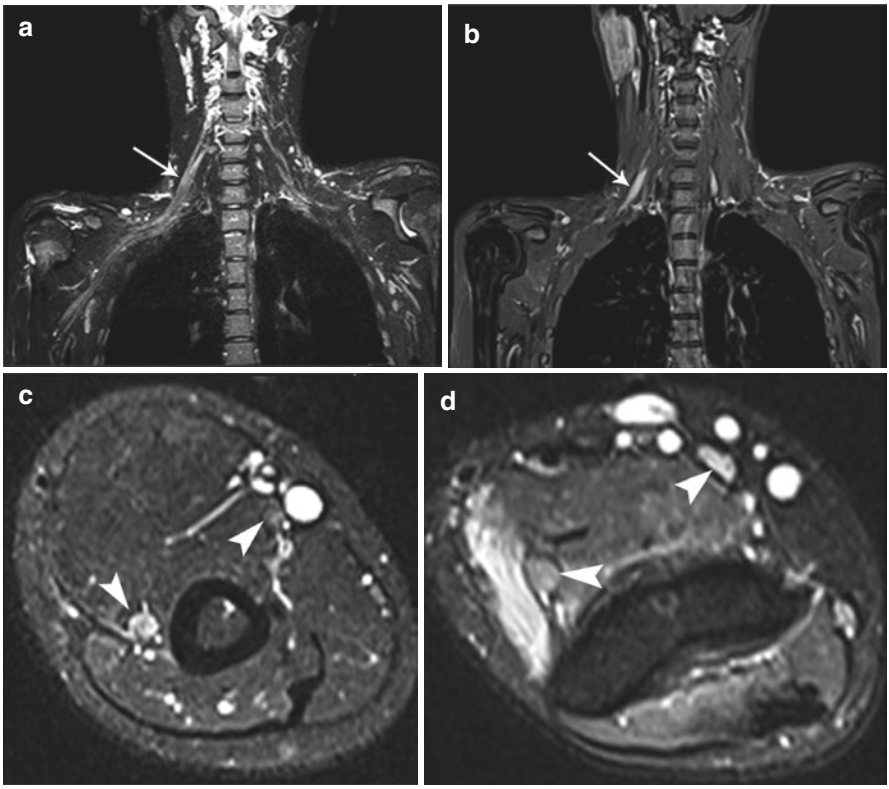

Fig. 5.9 MADSAM, 3D MRN (1.5T) of the brachial plexus (**a**), coronal T1-W section after gadolinium administration (**b**), 2D MRN, axial T2-STIR section of the right arm (**c**, **d**). Asymmetric hypertrophy of the right brachial plexus (arrow in **a**), with enhancement of the right C6 nerve root and superior primary trunk (arrow in **b**). Hypertrophy and increased signal intensity of the right radial and median nerves (arrowheads in **c** and **d**)

Sensory predominant CIDP occurs in 5–35% of patients, often starting with lower limb numbness [43]. The diagnosis is typically made on the basis of demyelinating electrodiagnostic features in motor nerves, which may occur without motor signs, although patients may develop weakness at a later date [44]. This entity may be under-diagnosed at the onset of symptoms which manifest at a young age and 3D MRN may represent a useful diagnostic tool when demonstrating symmetric hypertrophy of the brachial and lumbosacral plexus, which is comparable to the typical form of CIDP [45].

Recent comparative studies showed that both MRI and high-resolution sonography (HRUS) of the brachial plexus can be used to support the clinical suspicion of an inflammatory neuropathy [46]. HRUS appears to be more sensitive for nerve (root) thickening, whereas MRI complements this with an abnormal T2 signal. An increased T2 signal has been reported to be more frequently found in patients with CIDP than Multifocal Motor Neuropathy (MMN).

Brachial and lumbosacral plexus hypertrophy on MRI is also well documented in patients with demyelinating Charcot–Marie–Tooth disease (CMT) [47] and the differential diagnosis with CIDP, besides genetic abnormalities, can also rely on the measurement of the sciatic nerve cross-sectional area (CSA) at mid-thigh by means of MRN [48] (Fig. 5.10).

New MR techniques such as diffusion-weighted (DWI) and diffusion tensor (DTI) imaging have proven to be particularly useful for the investigation of CIDP.

High signal intensity in DWI sequences and increased values of the apparent diffusion coefficient (ADC) were detected in 55.6% of cases in a small cohort of 13 CIDP patients, which might be strictly correlated with proliferating layers of Schwann cells and increased endoneurial collagen surrounding the axons [49].

With the clinical availability of 3T MR units, DTI is increasingly used to detect microstructural abnormalities of nerves in CIDP patients.

FA has been shown to be significantly reduced in tibial nerves of patients with variable disease duration, correlating with the amplitude of compound motor action potentials, thus with the axonal damage [50], whereas RD is increased in nerves of CIDP patients and may represent a specific biomarker of demyelinating neuropathy, inversely correlated with nerve conduction velocities (NCV) [51].

DTI may reveal low FA in sciatic nerves that are correlated with clinical impairment in CIDP patients treated with subcutaneous immunoglobulin, in whom MRN is unable to identify abnormalities [52].

These preliminary results suggest a role of DTI as a research tool for identifying quantitative measure of microstructural abnormalities, although further testing is needed to validate the method (Fig. 5.8d).

5.4.2 Multifocal Motor Neuropathy

Multifocal motor neuropathy (MMN) is a chronic, immune-mediated demyelinating neuropathy, affecting motor fibers, characterized by progressive, predominantly distal, asymmetric limb weakness, mostly affecting upper limbs, minimal or no

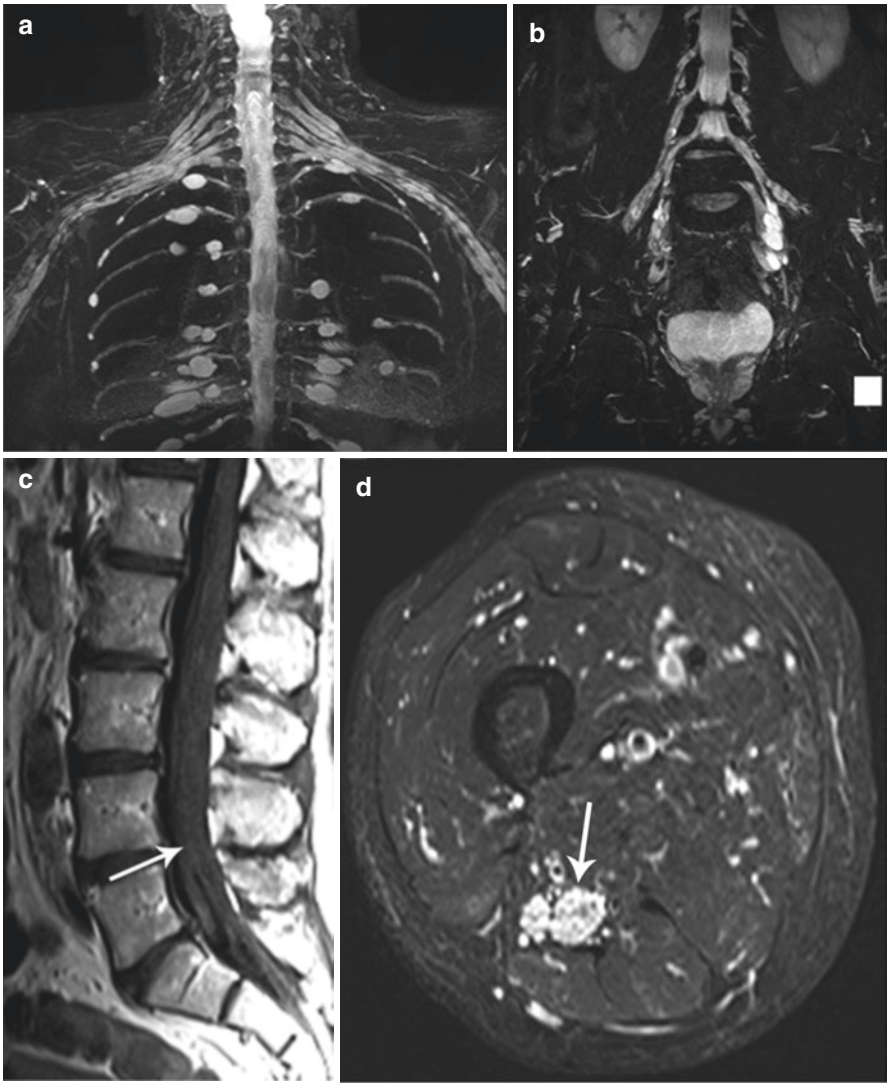

Fig. 5.10 CMT 1A, 3D MRN (1.5T) (**a**, **b**), sagittal T1-W section of the lumbar spine (**c**), axial MRN, T2-STIR section at mid-thigh (**d**). Diffuse symmetric hypertrophy and hyperintensity of the brachial plexus and intercostal nerves (**a**) and lumbosacral plexus (**b**). Hypertrophy of the cauda equina (arrow in **c**). Hyperintensity and hypertrophy of the right sciatic nerve (CSA = 270 mm^2) (arrow), with excellent visualization of the tibial and peroneal divisions

sensory impairment, and the presence of multifocal persistent partial conduction blocks (CB) on motor nerves [53]. Increased levels of serum IgM antibodies to the ganglioside GM1 is another typical feature of the disease.

MRI may be of value in the differential diagnosis between CIDP and MMN, classified as a variant of CIDP in the past and now considered a different disease [54].

A recent revision of the European Federation of Neurological Societies/Peripheral Nerve Society on Multifocal Motor Neuropathies (MMN) also included MRI as a supportive criterion for the differential diagnosis with other neuropathies such as CIDP or multifocal acquired demyelinating sensory and motor (MADSAM) neuropathy (Lewis-Sumner syndrome) and motor neuron disease (MND) [55].

About 40–50% of the patients with MMN show asymmetric hypertrophy and signal intensity abnormalities or contrast-enhancement on MR of the brachial plexus and the pattern of signal alterations closely correlates with the distribution of muscle weakness [56] (Fig. 5.11).

Diffuse nerve swelling and hyperintensity of the affected nerves on the T2-weighted images are usually found in areas outside the expected confines of entrapment neuropathy and reflect demyelination and proximal conduction blocks [57].

The clinical presentation of MMN may mimic motor neuron disease (MND), particularly in patients with predominant lower motor neuron impairment and the differential diagnosis is important, as the prognosis and treatment of these diseases are different.

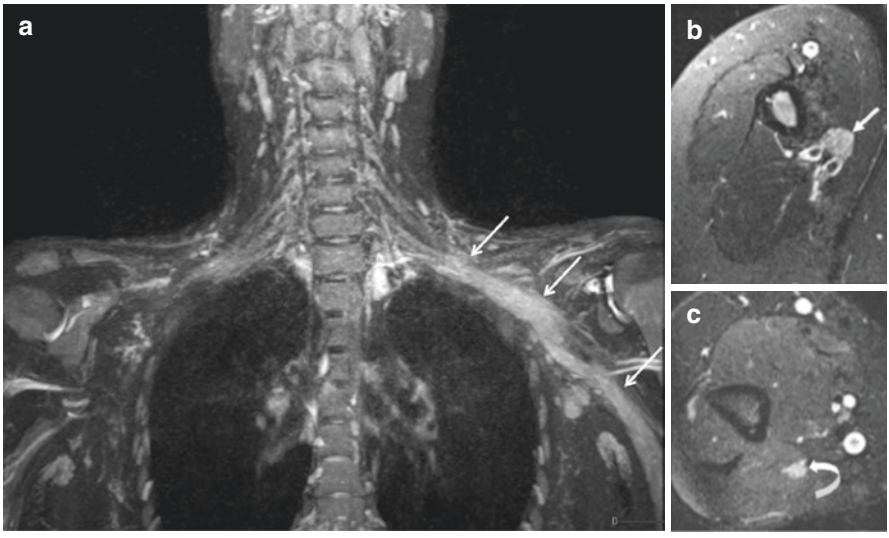

Fig. 5.11 MMN, 3D MRN (1.5T) of the brachial plexus (**a**), axial 2D MRN at mid-arm (**b**), and elbow (**c**). Asymmetric hypertrophy and hyperintensity of the left brachial plexus with prevalent involvement of the trunks and cords (arrows in **a**). Hypertrophy and hyperintensity of the left median (arrow in **b**) and ulnar nerves (curved arrow in **c**)

MRI can be used to help differentiate between MMN and MND, with brachial plexus MRI being normal in the latter [58].

High-resolution ultrasound can provide complementary information to MRI, showing significantly increased cross-sectional area values of the median and ulnar nerve in the forearm in patients with MMN as compared to MND [59].

DTI has been recently demonstrated to be useful for the differential diagnosis between MMN and MND. Besides the known enlargement of median and ulnar nerves, AD values of median and ulnar nerves at forearm arm are significantly lower in MMN patients compared to MND patients and healthy controls, especially in the proximal segments [60]. Thickening of nerves is compatible with changes in the myelin sheath structure, whereas lowered AD values suggest axonal dysfunction.

Axonal multifocal motor neuropathy is a rare entity, which was first described in 2002, and is characterized by a slowly progressive multifocal motor phenotype with neither conduction blocks nor other features of demyelination [61].

MR Neurography has been recently reported to be helpful in the diagnostic workup of the axonal form of MMN, showing mildly increased signal intensity and size of the involved nerves at the arm [62].

5.5 Diabetic Polyneuropathy

Diabetic peripheral neuropathy (DPN) is the most common form of the diabetic neuropathies seen in either type 1 (T1D) or type 2 (T1D) Diabetes Mellitus, with similar frequency. DPN is a common late complication of diabetes and has been defined as a symmetric, length-dependent sensorimotor polyneuropathy attributable to metabolic and microvascular alterations as a result of chronic hyperglycemia exposure and cardiovascular risk covariates [63]. Diabetic neuropathy is believed to be related to damage to the vascular supply of the nerves (vasa nervosa) and/or deposition of advanced glycosylation products in the intraneural space [64].

A combined MRN and DTI MR investigation at 3 Tesla has demonstrated larger sciatic nerve volume and multifocal fascicular lesions in diabetic patients with polyneuropathy with higher neuropathy deficit score (NDS), as compared to non-neuropathic diabetic patients and healthy control subjects [65]. Lower FA and higher MD and RD were found in sciatic nerves of patients with DPN compared with both non-neuropathic patients and healthy controls, correlating closely with the severity of neuropathy, and possibly reflecting loss of axons and/or myelin.

According to a recent MR study, the predominant type of nerve lesion in the sciatic nerves of patients with DPN differs between T1D and T2D [66]. An increased volume of T2w-hyperintense lesions is observed in T1D compared to T2D, whereas T2w-hypointense lesion volume is higher in T2D compared to T1D. Predominant nerve lesions in T1D are associated with poor glycemic control and loss of nerve conduction, whereas predominant lesions in T2D are associated with changes in lipid metabolism.

DPN includes diabetic radiculoplexus neuropathies also known as diabetic amyotrophy, which affect roots, plexus, and individual nerves in the cervical, thoracic, or lumbosacral segments.

Diabetic lumbosacral radiculoplexus neuropathy (DLRPN), which is characterized by debilitating pain, weakness, atrophy of the proximal thigh muscles, and abnormal protein content in CSF, is the best studied subtype [67].

MR imaging is very useful in demonstrating increased signal intensity in nerve roots and trunks which is invariably associated to denervation changes in the affected muscles [68].

The occurrence of a cervical diabetic radiculoplexus neuropathy (DCRPN) sharing many of the clinical and pathological features of DLRPN has also been demonstrated [69] (Fig. 5.12).

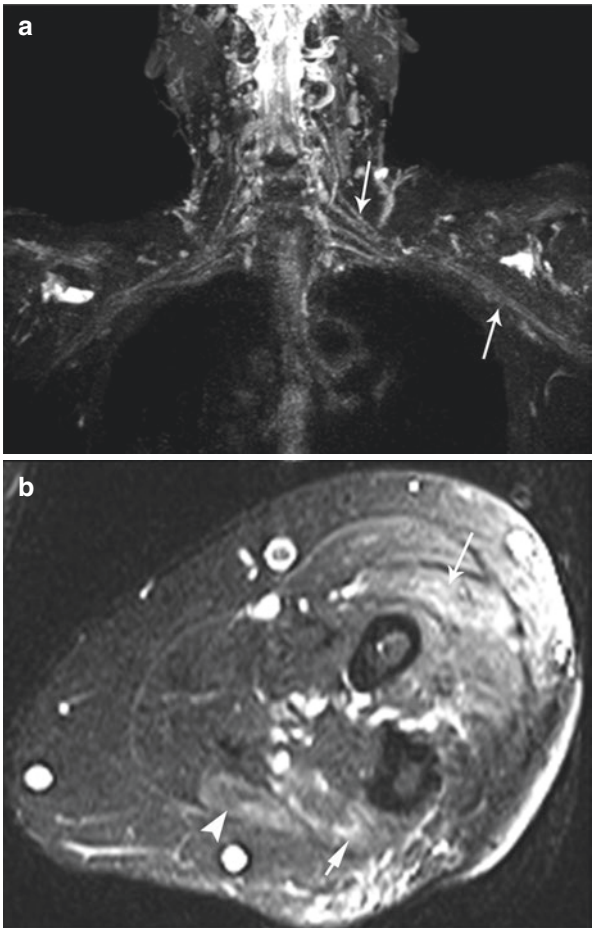

Fig. 5.12 Diabetic cervical radiculoplexus neuropathy in a 64-year-old female with type 2 diabetes, 3D MRN (1.5T) (**a**), 2D MRN, axial T2-STIR section at left mid-forearm (**b**). Mild enlargement and hyperintensity of the left supra and infraclavear brachial plexus (arrows). Denervation changes into the left extensor carpi ulnaris (short arrow), extensor digitorum (arrowhead), and extensor carpi radialis (long arrow)

5.6 Amyloid Neuropathy

Amyloid neuropathies occur in a context of hereditary or acquired amyloidosis. They present usually as severe and progressive polyneuropathy involving sensory, motor, and/or autonomic fibers and carry a poor prognosis [70].

Acquired amyloid neuropathy is almost exclusively represented by immunoglobulin light chain amyloidosis (AL) and is frequently associated with renal manifestations and monoclonal protein

in serum or urine. Peripheral neuropathy occurs in about 35% of cases of AL but is a rare presenting symptom [71].

On MR imaging, both focal amyloidoma or diffuse enlargement of unilateral/bilateral nerves with associated multifocal lesions have been reported [30, 72].

The lesions most commonly involve segments of the lumbosacral plexus or the sciatic nerve and are characterized by increased nerve T2 signal of the affected nerves, with a proximal-to-distal gradient, correlating with the clinical severity [30].

Transthyretin familial amyloid polyneuropathy (TTR-FAP) is the most common form of inherited amyloidosis. Endemic areas of TTR-FAP are Portugal, Japan, Sweden, and Brazil. Patients with FAP may experience different patterns of neuropathy including focal neuropathies, sensorimotor polyneuropathy, autonomic neuropathy, or combinations of the three. The median nerve at the wrist is a common and early site of involvement in FAP [73].

The diagnosis relies on a positive family history and requires TTR gene analysis showing Met30TTR mutation and positive labial salivary gland biopsy (LSGB) for amyloidosis [74].

High-resolution 3T MRN has been recently shown to be able to identify and quantify the distribution of peripheral nerve injury in TTR-FAP patients within the fascicles of the sciatic nerves from proximal to distal (Fig. 5.13), even before

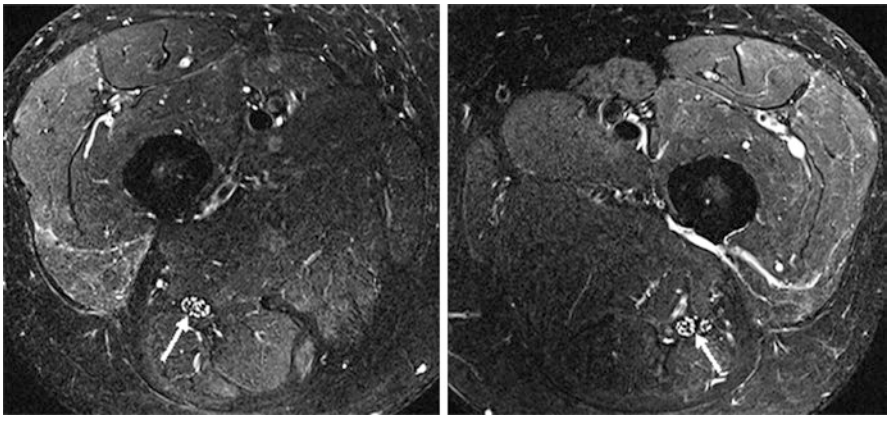

Fig. 5.13 Transthyretin familial amyloid polyneuropathy. 2D MRN at proximal thigh, showing increased signal intensity and mild increase of the fascicular size of both sciatic nerves (arrows)

the manifestation of symptomatic disease in asymptomatic gene carriers, in whom imaging detection may precede clinical and electrophysiological manifestation [75].

5.7 Sarcoidosis

Sarcoidosis is a granulomatous, multisystem disease of unknown etiology. Approximately 3.5–5% of the patients with sarcoidosis have involvement of the central and peripheral nervous system (Neurosarcoidosis) although peripheral nerve manifestations are rare and usually seen late in the disease.

Acute or chronic peripheral neuropathy occurs in about 2–40% of patients with neurosarcoidosis. The most common form is represented by symmetrical axonal sensory motor polyneuropathy. Other patterns include mononeuritis multiplex and Guillain-Barre-like syndrome [76].

Sarcoid granulomas locate themselves in the perineurium and epineurium, while the endoneurium is mostly spared.

Although CNS sarcoidosis can be diagnosed using contrast-enhanced MR imaging [77], the diagnosis of PNS sarcoidosis is more difficult.

MRN has been reported as a useful tool in the diagnostic workup of sciatic nerve sarcoidosis, which can manifest as a mass within the sciatic nerve (sarcoid granuloma), characterized by low signal intensity in T2-weighted images and marked enhancement after contrast administration [78].

Key Points

- Magnetic Resonance Neurography is an imaging technique, directed at identifying and evaluating specific characteristics of nerve morphology, such as internal fascicular pattern, and longitudinal variations in signal intensity and caliber.
- Advanced 3D MR Neurography techniques allow oblique and curved-planar reformations along the course of peripheral nerves and are particularly suitable for imaging brachial and lumbosacral plexus.
- Diseased nerves are hyperintense to muscle on MRN images and appear focally or globally enlarged. The signal intensity variations are not specific and are due to increased water content in the epineurial space, blockade of axoplasmic flow, inflammation and distal Wallerian degeneration.
- Muscle denervation imaging is part of an MR Neurography examination and represents a useful sign of peripheral nerve disease.
- The most frequent MRI finding in patients affected by CIDP is represented by bilateral and symmetric hypertrophy and hyperintensity of both brachial and lumbosacral plexus, better displayed by MR Neurography.
- Atypical variants of CIDP and MMN can be noninvasively characterized with 3D MRN of the brachial and lumbosacral plexus, showing symmetric or asymmetric longitudinal morphological changes from roots to nerve trunks and variable contrast-enhancement.

- DTI provides quantitative measurements of some microstructural properties of peripheral nerves, which are potentially useful for more precise imaging characterization of immune-mediated neuropathies.
- MRI of the brachial plexus can be used in the differential diagnosis between MMN and MND, with MRI being normal in the latter.
- In diabetic cervical and lumbosacral radiculoplexus neuropathies MR Neurography is useful in demonstrating increased signal intensity in nerve roots and trunks which is invariably associated to denervation changes into the affected muscles.

References

1. Pullman SL, Goodin DS, Marquinez AI, Tabbal S, Rubin M. Clinical utility of surface EMG: report of the therapeutics and technology assessment subcommittee of the American Academy of Neurology. Neurology. 2000;55(2):171–7.
2. Khadilkar SV, Yadav RS, Soni G. A practical approach to enlargement of nerves, plexuses and roots. Pract Neurol. 2015;15(2):105–15.
3. Pham M, Baumer T, Bendszus M. Peripheral nerves and plexus: imaging by MR-neurography and high-resolution ultrasound. Curr Opin Neurol. 2014;27(4):370–9.
4. Filler AG, Howe FA, Hayes CE, et al. Magnetic resonance neurography. Lancet. 1993;341(8846):659–61.
5. Maravilla KR, Bowen BC. Imaging of the peripheral nervous system: evaluation of peripheral neuropathy and plexopathy. AJNR Am J Neuroradiol. 1998;19(6):1011–23.
6. Naraghi AM, Awdeh H, Wadhwa V, Andreisek G, Chhabra A. Diffusion tensor imaging of peripheral nerves. Semin Musculoskelet Radiol. 2015;19(2):191–200.
7. Padua L, Liotta G, Di PA, et al. Contribution of ultrasound in the assessment of nerve diseases. Eur J Neurol. 2012;19(1):47–54.
8. Filler AG, Maravilla KR, Tsuruda JS. MR neurography and muscle MR imaging for image diagnosis of disorders affecting the peripheral nerves and musculature. Neurol Clin. 2004;22(3):643–82, vi–vii
9. Chhabra A, Flammang A, Padua A Jr, Carrino JA, Andreisek G. Magnetic resonance neurography: technical considerations. Neuroimaging Clin N Am. 2014;24(1):67–78.
10. Thawait SK, Chaudhry V, Thawait GK, et al. High-resolution MR neurography of diffuse peripheral nerve lesions. AJNR Am J Neuroradiol. 2011;32(8):1365–72.
11. Vargas MI, Viallon M, Nguyen D, Beaulieu JY, Delavelle J, Becker M. New approaches in imaging of the brachial plexus. Eur J Radiol. 2010;74(2):403–10.
12. Oudeman J, Coolen BF, Mazzoli V, et al. Diffusion-prepared neurography of the brachial plexus with a large field-of-view at 3T. J Magn Reson Imaging. 2016;43(3):644–54.
13. Sneag DB, Queler S. Technological advancements in magnetic resonance neurography. Curr Neurol Neurosci Rep. 2019;19(10):75.
14. Stoll G, Bendszus M, Perez J, Pham M. Magnetic resonance imaging of the peripheral nervous system. J Neurol. 2009;256(7):1043–51.
15. Chappell KE, Robson MD, Stonebridge-Foster A, et al. Magic angle effects in MR neurography. AJNR Am J Neuroradiol. 2004;25(3):431–40.
16. Aagaard BD, Maravilla KR, Kliot M. Magnetic resonance neurography: magnetic resonance imaging of peripheral nerves. Neuroimaging Clin N Am. 2001;11(1):viii, 131-146
17. Peled S, Cory DG, Raymond SA, Kirschner DA, Jolesz FA. Water diffusion, T(2), and compartmentation in frog sciatic nerve. Magn Reson Med. 1999;42(5):911–8.

18. Tanaka K, Mori N, Yokota Y, Suenaga T. MRI of the cervical nerve roots in the diagnosis of chronic inflammatory demyelinating polyradiculoneuropathy: a single-institution, retrospective case-control study. BMJ Open. 2013;3(8):e003443.
19. Bendszus M, Koltzenburg M, Wessig C, Solymosi L. Sequential MR imaging of denervated muscle: experimental study. AJNR Am J Neuroradiol. 2002;23(8):1427–31.
20. Jeon T, Fung MM, Koch KM, Tan ET, Sneag DB. Peripheral nerve diffusion tensor imaging: overview, pitfalls, and future directions. J Magn Reson Imaging. 2018;47(5):1171–89.
21. Breitenseher JB, Kranz G, Hold A, et al. MR neurography of ulnar nerve entrapment at the cubital tunnel: a diffusion tensor imaging study. Eur Radiol. 2015;25(7):1911–8.
22. Jengojan S, Kovar F, Breitenseher J, Weber M, Prayer D, Kasprian G. Acute radial nerve entrapment at the spiral groove: detection by DTI-based neurography. Eur Radiol. 2015;25(6):1678–83.
23. Wang H, Ma J, Zhao L, Wang Y, Jia X. Utility of MRI diffusion tensor imaging in carpal tunnel syndrome: a meta-analysis. Med Sci Monit. 2016;22:736–42.
24. Chhabra A, Ahlawat S, Belzberg A, Andreseik G. Peripheral nerve injury grading simplified on MR neurography: as referenced to Seddon and Sunderland classifications. Indian J Radiol Imaging. 2014;24(3):217–24.
25. Bowley MP, Doughty CT. Entrapment neuropathies of the lower extremity. Med Clin North Am. 2019;103(2):371–82.
26. Doughty CT, Bowley MP. Entrapment neuropathies of the upper extremity. Med Clin North Am. 2019;103(2):357–70.
27. Ahlawat S, Chhabra A, Blakely J. Magnetic resonance neurography of peripheral nerve tumors and tumorlike conditions. Neuroimaging Clin N Am. 2014;24(1):171–92.
28. Trivedi JR, Phillips L, Chhabra A. Hereditary and acquired polyneuropathy conditions of the peripheral nerves: clinical considerations and MR neurography imaging. Semin Musculoskelet Radiol. 2015;19(2):130–6.
29. Jende JME, Groener JB, Kender Z, et al. Structural nerve remodeling at 3-T MR Neurography differs between painful and painless diabetic polyneuropathy in type 1 or 2 diabetes. Radiology. 2020;294(2):405–14.
30. Kollmer J, Weiler M, Purrucker J, et al. MR neurography biomarkers to characterize peripheral neuropathy in AL amyloidosis. Neurology. 2018;91(7):e625–34.
31. Fujimura H. The Guillain-Barre syndrome. Handb Clin Neurol. 2013;115:383–402.
32. Vucic S, Kiernan MC, Cornblath DR. Guillain-Barre syndrome: an update. J Clin Neurosci. 2009;16(6):733–41.
33. van den Berg B, Walgaard C, Drenthen J, Fokke C, Jacobs BC, van Doorn PA. Guillain-Barre syndrome: pathogenesis, diagnosis, treatment and prognosis. Nat Rev Neurol. 2014;10(8):469–82.
34. Byun WM, Park WK, Park BH, Ahn SH, Hwang MS, Chang JC. Guillain-Barre syndrome: MR imaging findings of the spine in eight patients. Radiology. 1998;208(1):137–41.
35. Anadani M, Katirji B. Acute-onset chronic inflammatory demyelinating polyneuropathy: an electrodiagnostic study. Muscle Nerve. 2015;52(5):900–5.
36. Mathey EK, Park SB, Hughes RA, et al. Chronic inflammatory demyelinating polyradiculoneuropathy: from pathology to phenotype. J Neurol Neurosurg Psychiatry. 2015;86(9):973–85.
37. Rajabally YA, Chavada G. Lewis-Sumner syndrome of pure upper-limb onset: diagnostic, prognostic, and therapeutic features. Muscle Nerve. 2009;39(2):206–20.
38. Van den Bergh PY, Hadden RD, Bouche P, et al. European Federation of Neurological Societies/Peripheral Nerve Society guideline on management of chronic inflammatory demyelinating polyradiculoneuropathy: report of a joint task force of the European Federation of Neurological Societies and the Peripheral Nerve Society—first revision. Eur J Neurol. 2010;17(3):356–63.
39. Duggins AJ, McLeod JG, Pollard JD, et al. Spinal root and plexus hypertrophy in chronic inflammatory demyelinating polyneuropathy. Brain. 1999;122(Pt 7):1383–90.

40. Kuwabara S, Nakajima M, Matsuda S, Hattori T. Magnetic resonance imaging at the demyelinative foci in chronic inflammatory demyelinating polyneuropathy. Neurology. 1997;48(4):874–7.
41. Shibuya K, Sugiyama A, Ito S, et al. Reconstruction magnetic resonance neurography in chronic inflammatory demyelinating polyneuropathy. Ann Neurol. 2015;77(2):333–7.
42. Lozeron P, Lacour MC, Vandendries C, et al. Contribution of plexus MRI in the diagnosis of atypical chronic inflammatory demyelinating polyneuropathies. J Neurol Sci. 2016;360:170–5.
43. Ayrignac X, Viala K, Koutlidis RM, et al. Sensory chronic inflammatory demyelinating polyneuropathy: an under-recognized entity? Muscle Nerve. 2013;48(5):727–32.
44. van Dijk GW, Notermans NC, Franssen H, Wokke JH. Development of weakness in patients with chronic inflammatory demyelinating polyneuropathy and only sensory symptoms at presentation: a long-term follow-up study. J Neurol. 1999;246(12):1134–9.
45. Gasparotti R, Lucchetta M, Cacciavillani M, et al. Neuroimaging in diagnosis of atypical polyradiculoneuropathies: report of three cases and review of the literature. J Neurol. 2015;262(7):1714–23.
46. Goedee HS, Jongbloed BA, van Asseldonk JH, et al. A comparative study of brachial plexus sonography and magnetic resonance imaging in chronic inflammatory demyelinating neuropathy and multifocal motor neuropathy. Eur J Neurol. 2017;24(10):1307–13.
47. Ellegala DB, Monteith SJ, Haynor D, Bird TD, Goodkin R, Kliot M. Characterization of genetically defined types of Charcot-Marie-Tooth neuropathies by using magnetic resonance neurography. J Neurosurg. 2005;102(2):242–5.
48. Sinclair CD, Miranda MA, Cowley P, et al. MRI shows increased sciatic nerve cross sectional area in inherited and inflammatory neuropathies. J Neurol Neurosurg Psychiatry. 2011;82(11):1283–6.
49. Adachi Y, Sato N, Okamoto T, et al. Brachial and lumbar plexuses in chronic inflammatory demyelinating polyradiculoneuropathy: MRI assessment including apparent diffusion coefficient. Neuroradiology. 2011;53(1):3–11.
50. Kakuda T, Fukuda H, Tanitame K, et al. Diffusion tensor imaging of peripheral nerve in patients with chronic inflammatory demyelinating polyradiculoneuropathy: a feasibility study. Neuroradiology. 2011;53(12):955–60.
51. Kronlage M, Pitarokoili K, Schwarz D, et al. Diffusion tensor imaging in chronic inflammatory demyelinating polyneuropathy: diagnostic accuracy and correlation with electrophysiology. Invest Radiol. 2017;52(11):701–7.
52. Markvardsen LH, Vaeggemose M, Ringgaard S, Andersen H. Diffusion tensor imaging can be used to detect lesions in peripheral nerves in patients with chronic inflammatory demyelinating polyneuropathy treated with subcutaneous immunoglobulin. Neuroradiology. 2016;58(8):745–52.
53. Nobile-Orazio E, Gallia F. Multifocal motor neuropathy: current therapies and novel strategies. Drugs. 2013;73(5):397–406.
54. Vlam L, van der Pol WL, Cats EA, et al. Multifocal motor neuropathy: diagnosis, pathogenesis and treatment strategies. Nat Rev Neurol. 2011;8(1):48–58.
55. Joint Task Force of the EFNS and the PNS. European Federation of Neurological Societies/Peripheral Nerve Society guideline on management of multifocal motor neuropathy. Report of a joint task force of the European Federation of Neurological Societies and the Peripheral Nerve Society—first revision. J Peripher Nerv Syst. 2010;15(4):295–301.
56. Van Asseldonk JT, Van den Berg LH, Van den Berg-Vos RM, Wieneke GH, Wokke JH, Franssen H. Demyelination and axonal loss in multifocal motor neuropathy: distribution and relation to weakness. Brain. 2003;126(Pt 1):186–98.
57. van Es HW, Van den Berg LH, Franssen H, et al. Magnetic resonance imaging of the brachial plexus in patients with multifocal motor neuropathy. Neurology. 1997;48(5):1218–24.
58. Van Den Berg-Vos RM, Van Den Berg LH, Visser J, de Visser M, Franssen H, Wokke JH. The spectrum of lower motor neuron syndromes. J Neurol. 2003;250(11):1279–92.

59. Jongbloed BA, Haakma W, Goedee HS, et al. Comparative study of peripheral nerve Mri and ultrasound in multifocal motor neuropathy and amyotrophic lateral sclerosis. Muscle Nerve. 2016;54(6):1133–5.
60. Haakma W, Jongbloed BA, Froeling M, et al. MRI shows thickening and altered diffusion in the median and ulnar nerves in multifocal motor neuropathy. Eur Radiol. 2017;27(5):2216–24.
61. Katz JS, Barohn RJ, Kojan S, et al. Axonal multifocal motor neuropathy without conduction block or other features of demyelination. Neurology. 2002;58(4):615–20.
62. Briani C, Cacciavillani M, Lucchetta M, Cecchin D, Gasparotti R. MR neurography findings in axonal multifocal motor neuropathy. J Neurol. 2013;260(9):2420–2.
63. Tesfaye S, Boulton AJ, Dyck PJ, et al. Diabetic neuropathies: update on definitions, diagnostic criteria, estimation of severity, and treatments. Diabetes Care. 2010;33(10):2285–93.
64. Van Dam PS, Cotter MA, Bravenboer B, Cameron NE. Pathogenesis of diabetic neuropathy: focus on neurovascular mechanisms. Eur J Pharmacol. 2013;719(1–3):180–6.
65. Vaeggemose M, Pham M, Ringgaard S, et al. Magnetic resonance neurography visualizes abnormalities in sciatic and tibial nerves in patients with type 1 diabetes and neuropathy. Diabetes. 2017;66(7):1779–88.
66. Jende JME, Groener JB, Oikonomou D, et al. Diabetic neuropathy differs between type 1 and type 2 diabetes: insights from magnetic resonance neurography. Ann Neurol. 2018;83(3):588–98.
67. Dyck PJ, Norell JE, Dyck PJ. Microvasculitis and ischemia in diabetic lumbosacral radiculoplexus neuropathy. Neurology. 1999;53(9):2113–21.
68. Hlis R, Poh F, Bryarly M, Xi Y, Chhabra A. Quantitative assessment of diabetic amyotrophy using magnetic resonance neurography—a case-control analysis. Eur Radiol. 2019;29(11):5910–9.
69. Massie R, Mauermann ML, Staff NP, et al. Diabetic cervical radiculoplexus neuropathy: a distinct syndrome expanding the spectrum of diabetic radiculoplexus neuropathies. Brain. 2012;135(Pt 10):3074–88.
70. Adams D, Lozeron P, Lacroix C. Amyloid neuropathies. Curr Opin Neurol. 2012;25(5):564–72.
71. Shin SC, Robinson-Papp J. Amyloid neuropathies. Mt Sinai J Med. 2012;79(6):733–48.
72. Kanta M, Ehler E, Kohout A, et al. Rare case of a localized radial nerve amyloid neuropathy. J Clin Neuromuscul Dis. 2014;16(1):20–3.
73. Koyama S, Kawanami T, Kurokawa K, et al. Carpal tunnel syndrome as an initial manifestation in a case of transthyretin-related familial amyloid polyneuropathy with a novel A120T mutation. Clin Neurol Neurosurg. 2012;114(6):707–9.
74. Adams D, Suhr OB, Hund E, et al. First European consensus for diagnosis, management, and treatment of transthyretin familial amyloid polyneuropathy. Curr Opin Neurol. 2016;29(Suppl 1):S14–26.
75. Kollmer J, Hund E, Hornung B, et al. In vivo detection of nerve injury in familial amyloid polyneuropathy by magnetic resonance neurography. Brain. 2015;138(Pt 3):549–62.
76. Nozaki K, Judson MA. Neurosarcoidosis. Curr Treat Options Neurol. 2013;15(4):492–504.
77. Smith JK, Matheus MG, Castillo M. Imaging manifestations of neurosarcoidosis. AJR Am J Roentgenol. 2004;182(2):289–95.
78. Dailey AT, Rondina MT, Townsend JJ, Shrieve DC, Baringer JR, Moore KR. Sciatic nerve sarcoidosis: utility of magnetic resonance peripheral nerve imaging and treatment with radiation therapy. J Neurosurg. 2004;100(5):956–9.